

A fractional-order compartmental model for the Spread of the COVID-19 pandemic

T. A. Biala*, A. Q. M. Khaliq

*Center for Computational Science and Department of Mathematical Sciences,
Middle Tennessee State University,
Murfreesboro, TN 37132-0001, USA.*

Abstract

We propose a time-fractional compartmental model ($SEI_A I_S HRD$) comprising of the susceptible, exposed, infected (asymptomatic and symptomatic), hospitalized, recovered and dead population for the COVID-19 pandemic. We study the properties and dynamics of the proposed model. The conditions under which the disease-free and endemic equilibrium points are asymptotically stable are discussed. Furthermore, we study the sensitivity of the parameters and use the data from Tennessee state (as a case study) to discuss identifiability of the parameters of the model. The non-negative parameters in the model are obtained by solving inverse problems with empirical data from California, Florida, Georgia, Maryland, Tennessee, Texas, Washington and Wisconsin. The basic reproduction number is seen to be slightly above the critical value of one suggesting that stricter measures such as the use of face-masks, social distancing, contact tracing, and even longer stay-at-home orders need to be enforced in order to mitigate the spread of the virus. As stay-at-home orders are rescinded in some of these states, we see that the number of cases began to increase almost immediately and may continue to rise until the end of the year 2020 unless stricter measures are taken.

Keywords: Time-fractional model, SEIR model, COVID-19, Sensitivity analysis, Parameter estimation and identifiability.

1. Introduction

Fractional differential equations (FDEs) are used to model complex phenomena such as the modeling of memory-dependent phenomena (Di Giuseppe *et al.* [1], Baleanu *et al.* [2], Podlubny [3]), mechanical properties of materials (Caputo and Mainardi [4]), anomalous diffusion in porous media (Fomin *et al.* [5], Metzler and Klafter [6]), groundwater flow problems (Clout

Email addresses: *tab7v@mtmail.mtsu.edu (T. A. Biala*), Abdul.Khaliq@mtsu.edu (A. Q. M. Khaliq)

and Botha [7], Iaffaldano *et al.* [8]), and control theory (Podlubny [9]), among others. They serve as a generalization of the integer-order differential equations and give more degree of freedom for modeling of biological and physical processes. FDEs have been applied in biological tissues [10], DNA sequencing [11], Pine Wilt disease [12], lung tissue mechanics and models [13], harmonic oscillators [14], Dengue fever [15], measles [16], human liver [17], diffusion processes [18], SEIR models [19]. Infectious disease outbreaks are one of the main causes of deaths in human. Their dynamics and spread are modeled and studied before the introduction of vaccines. COVID-19 began in December 2019 in China. Over the last few months, it has spread rapidly leading to over 400,000 deaths across the globe. The first occurrence in the United States was seen around mid January in Washington [20] and has spread across America with over 100,000 deaths and 1.5 million infected. The pandemic has disrupted the day-to-day activities of the human life with over six million jobs lost in the United States. Several actions and measures have been taken by the federal, state and local governments to mitigate the spread of the pandemic. The most prominent measures taken include social distancing, testing, use of face-masks and contact tracing. It is important to model this pandemic in order to better understand the spread and dynamics as well as address the challenges of the pandemic. In short, mathematical models are important to guide the decisions of health and government officials.

The goal of this study is to examine and analyze the spread of the pandemic using a modification of the Susceptible-Exposed-Infected-Recovered (SEIR) model with a time-fractional derivative. The use of fractional derivatives in the model stems from the fact that the spread of infectious diseases depends not only on the current state but also on its past states (history or memory dependency). Additionally, time-fractional order models reduce errors resulting from neglect of parameters in models. We shall focus on some selected states in the US. We note that models that consider the US as a whole may be misleading and have limited applicability as different states have different economical and political perspectives which determines the different control strategies used for each state. For example, while some states such as Maryland, New Jersey, New York, Connecticut, among others, enforced the use of masks in public places and longer stay-at-home order [21], other states do not enforce these measures thereby allowing for a possibility of increase of infected individuals in such states. There have been several models for the study of the pandemic. Lu *et al.* [22] considered a fractional-order SEIHDR model which incorporates intercity movements. Liu *et al.* [23] studied the dynamics of the pandemic by considering asymptomatic and symptomatic infected populations separately. Giordano *et al.* [24] studied the COVID-19 epidemic with intervention strategies in Italy. They proposed a model consisting of different stages: susceptible, infected, diagnosed, ailing, recognized, threatened, healed and extinct. They further discuss the long time behavior of the populations in which the susceptible, healed and extinct population remains. Stella *et al.* [25] studied the role of asymptomatic individuals via complex networks. In particular, they formulated a model which aims at studying the interactions in the population by means of complex networks. They

further extended the model to a structured nonhomogenous version by means of the Watts-Strogatz complex network. Wu *et al.* [26] studied domestic and international spread of the pandemic by using different data sets. Zhao and Chen [27] discussed the dynamics of the pandemic by considering the Susceptible, unquarantined infected, quarantined infected and Confirmed infected (SUQC) model and parametrize the intervention effect of control measures. Zhang *et al.* [28] considered a fractional SEIR model with different order of the time-fractional derivative for each of the different population being studied. Tuan *et al.* [29] proposed a fractional-order model using the Caputo derivative for studying the transmission of COVID-19. They discussed the existence and uniqueness of solutions to the proposed model. They further used the generalized Adams-Bashforth-Moulton method for simulating the model. Bahloul *et al.* [30] proposed a fractional-order Susceptible-Exposed-Infected-Quarantined- Recovered-Death-Insusceptible (SEIQRDP) model for predicting the spread of COVID-19. The remainder of the paper is organized as follows: In section 2, we give some preliminary results and definitions from fractional Calculus. Furthermore, we discuss the formulation of the model by considering seven compartments: Susceptible-Exposed-Asymptomatic infected-Symptomatic infected, Hospitalized, Recovered and Dead populations (SEI_AI_SHRD). Section 3 details the properties and theoretical analysis of the model. Section 4 discusses the parameter sensitivity and identifiability analysis. In section 5, we applied the model to observed data for some selected states in the US. In particular, this section details solving several inverse problems for parameter estimation and computation of the basic reproduction number. Finally, we give some concluding remarks in Section 6.

2. Model Setup

2.1. Preliminaries

In this section, we present some preliminary results and definitions in fractional calculus.

Definition 2.1. [3] The gamma function $\Gamma(\alpha)$ is defined by the integral

$$\Gamma(\alpha) = \int_0^{\infty} e^{-x} x^{\alpha} dx$$

which converges in the right half of the complex plane $\text{Re}(z) > 0$.

Definition 2.2. [31] For any $t > 0$, the Caputo-fractional derivative of order α , ($n < \alpha \leq n + 1$) of a function $f(t)$ is defined as

$${}_{t_0}\mathcal{D}_t^{\alpha} f(t) = \frac{1}{\Gamma(n - \alpha)} \int_{t_0}^t (t - \tau)^{n - \alpha - 1} f^{(n)}(\tau) d\tau.$$

Definition 2.3. [3] The Mittag-Leffler function which generalizes the exponential function for fractional calculus is defined as

$$E_{\alpha, \beta}(z) = \sum_{k=0}^{\infty} \frac{z^k}{\Gamma(\alpha k + \beta)}, \quad \alpha \in \mathbb{R}^+, \quad z \in \mathbb{C}.$$

Remark 2.1.

More generally, the two parameter Mittag-Leffler function is defined as

$$E_{\alpha}(z) = \sum_{k=0}^{\infty} \frac{z^k}{\Gamma(\alpha k + \beta)}, \quad \alpha, \beta \in \mathbb{R}^+, \quad z \in \mathbb{C}.$$

It has the following properties:

1. $E_{\alpha, \beta}(z) = z E_{\alpha, \alpha + \beta}(z) + \frac{1}{\Gamma(\beta)}$.
2. ${}_0\mathcal{D}_t^{\alpha} e^{\lambda t} = t^{-\alpha} E_{1, 1-\alpha}(\lambda t)$.
3. ${}_0\mathcal{D}_t^{\alpha} E_{\alpha, 1}(\lambda t^{\alpha}) = \lambda E_{\alpha, 1}(\lambda t^{\alpha})$.

Definition 2.4. [32] A point x^* is said to be an equilibrium point of the system ${}_0\mathcal{D}_t^{\alpha} = f(t, x(t))$, $x(t_0) > 0$ if and only if $f(t, x^*(t)) = 0$.

Definition 2.5. [22] An equilibrium point x^* of the system ${}_0\mathcal{D}_t^{\alpha} x(t) = f(t, x(t))$, $x(t_0) > 0$ is said to be asymptotically stable if all the eigenvalues of the Jacobian matrix $J = \partial f / \partial x$, evaluated at the equilibrium point, satisfies $|\arg(\lambda_i)| > \frac{\alpha\pi}{2}$, where λ_i are the eigenvalues of J .

2.2. Model Formulation

The model discussed in this work is a modification of the SEIR model having three additional compartments. We consider a SEI_AI_SHRD compartmental model which comprises of the susceptible, exposed, infected (asymptomatic and symptomatic), hospitalized, recovered and dead population. We assume that the natural death and birth rates are the same. We further assume that deaths in the S and R compartments are due to natural deaths and deaths in the other compartments are as a result of the pandemic. The schema below shows the transmission flow of the model.

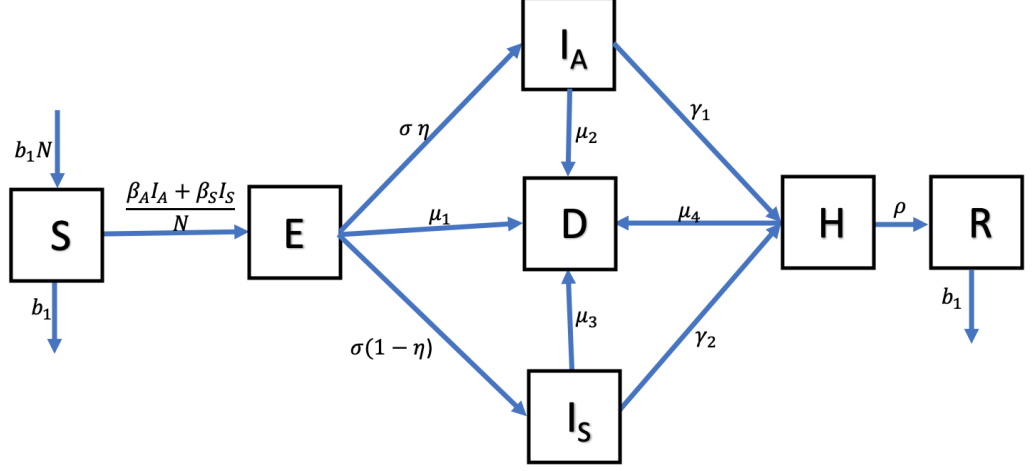


Figure 1: Schematic diagram of the proposed $SEI_A I_S HRD$ model

Thus, the model consists of the following system of ODEs

$$\begin{aligned}
{}_0\mathcal{D}_t^\alpha S(t) &= b_1 N - \frac{S(t)}{N} (\beta_A I_A(t) + \beta_S I_S(t)) - b_1 S(t), \\
{}_0\mathcal{D}_t^\alpha E(t) &= \frac{S(t)}{N} (\beta_A I_A(t) + \beta_S I_S(t)) - (\sigma + \mu_1) E(t), \\
{}_0\mathcal{D}_t^\alpha I_A(t) &= \eta \sigma E(t) - (\gamma_1 + \mu_2) I_A(t), \\
{}_0\mathcal{D}_t^\alpha I_S(t) &= (1 - \eta) \sigma E(t) - (\gamma_2 + \mu_3) I_S(t), \\
{}_0\mathcal{D}_t^\alpha H(t) &= \gamma_1 I_A(t) + \gamma_2 I_S(t) - (\rho + \mu_4) H(t), \\
{}_0\mathcal{D}_t^\alpha R(t) &= \rho H(t) - b_1 R(t), \\
{}_0\mathcal{D}_t^\alpha D(t) &= \mu_1 E(t) + \mu_2 I_A(t) + \mu_3 I_S(t) + \mu_4 H(t).
\end{aligned}$$

The system has the associated initial data

$$\begin{aligned}
S(0) &= S_0 \geq 0, & E(0) &= E_0 \geq 0, & I_A(0) &= I_{A0} \geq 0, \\
I_S(0) &= I_{S0} \geq 0, & H(0) &= H_0 \geq 0, & R(0) &= R_0 \geq 0, \\
D(0) &= D_0 \geq 0.
\end{aligned}$$

The total population is N which is further divided into $S(t)$, $E(t)$, $I_A(t)$, $I_S(t)$, $H(t)$ and $R(t)$, b_1 is the natural birth rate, β_A and β_S are the transmission rates to the susceptible population from the asymptomatic and symptomatic populations, respectively. $1/\sigma$ is the incubation period of an exposed individual, η denotes the fraction of the exposed population that becomes asymptomatic after the incubation period and the remaining $(1 - \eta)$ of the population are symptomatic. γ_1 and γ_2 are the infectious rates of an asymptomatic and a symptomatic individual, respectively. ρ is the recovery rate through hospitalization

and, μ_1 , μ_2 , μ_3 and μ_4 are the mortality rates of the exposed, asymptomatic, symptomatic and hospitalized populations, respectively. We note that the death population in the model comprises of deaths during exposure $\mu_1 E(t)$, infectious period ($\mu_2 I_A$ and $\mu_3 I_S$) and hospitalization $\mu_4 H$, and assume that deaths due to other natural occurrences are negligible for this populations.

We note that the parameters of the model are non-negative and have dimensions given by $1/\text{time}^\alpha$. This observation was originally noted in Diethelm [15]. To alleviate this difference in dimensions, we replace the parameters (except η) with a power α of new parameters to obtain the new system of equations

$$\begin{aligned}
{}_0\mathcal{D}_t^\alpha S(t) &= b_1^\alpha N - \frac{S(t)}{N} (\beta_A^\alpha I_A(t) + \beta_S^\alpha I_S(t)) - b_1^\alpha S(t), \\
{}_0\mathcal{D}_t^\alpha E(t) &= \frac{S(t)}{N} (\beta_A^\alpha I_A(t) + \beta_S^\alpha I_S(t)) - (\sigma^\alpha + \mu_1^\alpha) E(t), \\
{}_0\mathcal{D}_t^\alpha I_A(t) &= \eta \sigma^\alpha E(t) - (\gamma_1^\alpha + \mu_2^\alpha) I_A(t), \\
{}_0\mathcal{D}_t^\alpha I_S(t) &= (1 - \eta) \sigma^\alpha E(t) - (\gamma_2^\alpha + \mu_3^\alpha) I_S(t), \\
{}_0\mathcal{D}_t^\alpha H(t) &= \gamma_1^\alpha I_A(t) + \gamma_2^\alpha I_S(t) - (\rho^\alpha + \mu_4^\alpha) H(t), \\
{}_0\mathcal{D}_t^\alpha R(t) &= \rho^\alpha H(t) - b_1^\alpha R(t), \\
{}_0\mathcal{D}_t^\alpha D(t) &= \mu_1^\alpha E(t) + \mu_2^\alpha I_A(t) + \mu_3^\alpha I_S(t) + \mu_4^\alpha H(t).
\end{aligned} \tag{1}$$

3. Model Analysis

In this section, we discuss the properties of the model beginning with the existence, uniqueness, non-negativity and boundedness of solutions of the model (1). For simplicity in analysis, we reduce the system (1) to

$$\begin{aligned}
{}_0\mathcal{D}_t^\alpha S(t) &= b_1^\alpha N - \frac{S(t)}{N} (\beta_A^\alpha I_A(t) + \beta_S^\alpha I_S(t)) - b_1^\alpha S(t), \\
{}_0\mathcal{D}_t^\alpha E(t) &= \frac{S(t)}{N} (\beta_A^\alpha I_A(t) + \beta_S^\alpha I_S(t)) - (\sigma^\alpha + \mu_1^\alpha) E(t), \\
{}_0\mathcal{D}_t^\alpha I_A(t) &= \eta \sigma^\alpha E(t) - (\gamma_1^\alpha + \mu_2^\alpha) I_A(t), \\
{}_0\mathcal{D}_t^\alpha I_S(t) &= (1 - \eta) \sigma^\alpha E(t) - (\gamma_2^\alpha + \mu_3^\alpha) I_S(t), \\
{}_0\mathcal{D}_t^\alpha H(t) &= \gamma_1^\alpha I_A(t) + \gamma_2^\alpha I_S(t) - (\rho^\alpha + \mu_4^\alpha) H(t), \\
{}_0\mathcal{D}_t^\alpha R(t) &= \rho^\alpha H(t) - b_1^\alpha R(t),
\end{aligned} \tag{2}$$

since D is a linear combination of populations in some of the other compartments.

Theorem 3.1. *There exist a unique solution to the system (2) and the solution is non-negative and bounded for any given initial data $(S_0, E_0, I_{A0}, I_{S0}, H_0, R_0) \geq \mathbf{0} \in \mathbb{R}^6$.*

Proof. See Appendix A. □

3.1. Stability Analysis

3.1.1. Computation of the basic reproduction number R_0

We shall use the next generation matrix originally proposed by Diekmann *et al.* [33] and further elaborated on by van den Driesche and Watmough [34] and Diekmann *et al.* [35] to determine R_0 . The disease-free equilibrium point (DFE) is $(N, 0, 0, 0, 0, 0)$. Now, consider the four compartments $Y = (Y_1, Y_2, Y_3, Y_4) = (E, I_A, I_S, H)$ containing the infected individuals and let Y^* be the DFE point. Since the DFE point exists and is stable (shown in the next section) in the absence of any disease, then the linearized equation at the DFE is

$${}_0\mathcal{D}_t^\alpha Y_i = \mathcal{F}_i(Y) - \mathcal{V}_i(Y), \quad i = 1(1)4,$$

where $\mathcal{F}_i(Y)$ is the rate of appearance of new infections in compartment i and $\mathcal{V}_i(Y)$ is the rate of transfer of infections to and from compartment i . We further define

$$F = \frac{\partial \mathcal{F}(Y)}{\partial Y_j} \Big|_{Y=Y^*} \quad \text{and} \quad V = \frac{\partial \mathcal{V}_i(Y)}{\partial Y_j} \Big|_{Y=Y^*}, \quad i, j = 1(1)4.$$

Then $\rho(FV^{-1})$ is the basic reproduction number R_0 , where $\rho(x)$ is the spectral radius of x and FV^{-1} is the next generation matrix. For the system (2),

$$F = \begin{bmatrix} 0 & \beta_A^\alpha & \beta_S^\alpha & 0 \\ 0 & 0 & 0 & 0 \\ 0 & 0 & 0 & 0 \\ 0 & 0 & 0 & 0 \end{bmatrix}, \quad V = \begin{bmatrix} \sigma^\alpha + \mu_1^\alpha & 0 & 0 & 0 \\ -\eta\sigma^\alpha & \gamma_1^\alpha + \mu_2^\alpha & 0 & 0 \\ -(1-\eta)\sigma^\alpha & 0 & \gamma_2^\alpha + \mu_3^\alpha & 0 \\ 0 & -\gamma_1^\alpha & -\gamma_2^\alpha & (\rho^\alpha + \mu_4^\alpha) \end{bmatrix}$$

and the basic reproduction number is given as

$$R_0 = \frac{\sigma^\alpha [\eta\beta_A^\alpha(\gamma_2^\alpha + \mu_3^\alpha) + (1-\eta)\beta_S^\alpha(\gamma_1^\alpha + \mu_2^\alpha)]}{(\sigma^\alpha + \mu_1^\alpha)(\gamma_1^\alpha + \mu_2^\alpha)(\gamma_2^\alpha + \mu_3^\alpha)}. \quad (3)$$

Lemma 3.1. *The fractional system (2) has at most two equilibrium points*

1. a disease-free equilibrium point DFE = $(N, 0, 0, 0, 0, 0)$
2. an endemic equilibrium point EE = $(S^*, E^*, I_A^*, I_S^*, H^*, R^*)$,

where

$$\begin{aligned} S^* &= \frac{S_0}{R_0}, \\ E^* &= \frac{b_1^\alpha S_0}{R_0(\sigma^\alpha + \mu_1^\alpha)} \left(1 - \frac{1}{R_0}\right), \\ I_A^* &= \frac{\eta b_1^\alpha \sigma^\alpha S_0}{R_0(\sigma^\alpha + \mu_1^\alpha)(\gamma_1^\alpha + \mu_2^\alpha)} \left(1 - \frac{1}{R_0}\right), \\ I_S^* &= \frac{(1-\eta) b_1^\alpha \sigma^\alpha S_0}{R_0(\sigma^\alpha + \mu_1^\alpha)(\gamma_2^\alpha + \mu_3^\alpha)} \left(1 - \frac{1}{R_0}\right), \\ H^* &= \frac{b_1^\alpha \sigma^\alpha S_0}{R_0(\sigma^\alpha + \mu_1^\alpha)(\rho^\alpha + \mu_4^\alpha)} \left(1 - \frac{1}{R_0}\right) \left(\frac{\eta\gamma_1^\alpha}{\gamma_1^\alpha} + \frac{(1-\eta)\gamma_2^\alpha}{\gamma_2^\alpha + \mu_3^\alpha} \right), \\ R^* &= \frac{\rho^\alpha b_1^\alpha \sigma^\alpha S_0}{R_0(\sigma^\alpha + \mu_1^\alpha)(\rho^\alpha + \mu_4^\alpha)} \left(1 - \frac{1}{R_0}\right) \left(\frac{\eta\gamma_1^\alpha}{\gamma_1^\alpha} + \frac{(1-\eta)\gamma_2^\alpha}{\gamma_2^\alpha + \mu_3^\alpha} \right). \end{aligned}$$

Theorem 3.2. *The DFE point is locally asymptotically stable if $R_0 < 1$ and $K < 1$, where*

$$K = \frac{\sigma^\alpha [\eta \beta_A^\alpha (\sigma^\alpha + \gamma_1^\alpha + \mu_1^\alpha + \mu_2^\alpha) + (1 - \eta) \beta_S^\alpha (\sigma^\alpha + \gamma_2^\alpha + \mu_1^\alpha + \mu_3^\alpha)]}{(\sigma^\alpha + \gamma_1^\alpha + \mu_1^\alpha + \mu_2^\alpha) (\sigma^\alpha + \gamma_2^\alpha + \mu_1^\alpha + \mu_3^\alpha) (\gamma_1^\alpha + \gamma_2^\alpha + \mu_2^\alpha + \mu_2^\alpha)}.$$

Proof. See Appendix B. □

Theorem 3.3. *The EE point is locally asymptotically stable if $R_0 > 1$ and $(A_1 A_2 - A_3) A_3 \geq A_1^2 A_4$, where*

$$\begin{aligned} A_1 &= b_1^\alpha (2R_0 - 1) + R_0 (\sigma^\alpha + \gamma_1^\alpha + \gamma_2^\alpha + \mu_1^\alpha + \mu_2^\alpha + \mu_3^\alpha), \\ A_2 &= -\sigma^\alpha R_0 (\eta \beta_A^\alpha + (1 - \eta) \beta_S^\alpha) + b_1^\alpha R_0 (2R_0 - 1) (\sigma^\alpha + \gamma_1^\alpha + \gamma_2^\alpha + \mu_1^\alpha + \mu_2^\alpha + \mu_3^\alpha) \\ &\quad + R_0^2 [(\gamma_2^\alpha + \mu_3^\alpha) (\sigma^\alpha + \mu_1^\alpha) + (\gamma_2^\alpha + \mu_3) (\gamma_1^\alpha + \mu_2^\alpha) + (\sigma^\alpha + \mu_1^\alpha) (\gamma_1^\alpha + \mu_2^\alpha)], \\ A_3 &= b_1^{2\alpha} R_0^2 (2R_0 - 1) [(\gamma_2^\alpha + \mu_3^\alpha) (\sigma^\alpha + \mu_1^\alpha) + (\gamma_2^\alpha + \mu_3) (\gamma_1^\alpha + \mu_2^\alpha) + (\sigma^\alpha + \mu_1^\alpha) (\gamma_1^\alpha + \mu_2^\alpha)] \\ &\quad + R_0 (\sigma^\alpha + \mu_1^\alpha) (\gamma_1^\alpha + \mu_2^\alpha) (\gamma_2^\alpha + \mu_3) - \sigma^\alpha ((1 - \eta) (\gamma_1^\alpha + \mu_2^\alpha) \beta_S^\alpha + \eta (\gamma_2^\alpha + \mu_3^\alpha) \beta_A^\alpha), \\ A_4 &= b_1^{3\alpha} R_0^3 (2R_0 - 1) (\sigma^\alpha + \mu_1^\alpha) (\gamma_1^\alpha + \mu_2^\alpha) (\gamma_2^\alpha + \mu_3^\alpha) - \sigma^\alpha ((1 - \eta) \beta_S^\alpha (\gamma_1^\alpha + \mu_2^\alpha) \\ &\quad + \eta \beta_A^\alpha (\gamma_2^\alpha + \mu_3^\alpha))] \end{aligned}$$

Proof. See Appendix C. □

4. Parameter Sensitivity and Identifiability Analysis

We discuss the sensitivity and identifiability of the parameters with respect to the proposed model.

4.1. Sensitivity analysis

The sensitivity analysis (SA) deals with the significance or importance of the parameters in the model. In particular, it finds the most influential parameters that drives the dynamics of the model. It also describes the extent to which parameter changes affects the result of the methods or models with the goal of identifying the best set of parameters that describes the process or phenomena in question.

There are several SA methods which are broadly classified as local and global methods. In this work, we shall focus on the Morris screening method (local method) and Sobol analysis method (global method).

4.1.1. Morris Screening Method

The Morris screening method is a local sensitivity measure that makes use of the first order derivative of an output function $y = f(\theta) = f(\theta_1, \dots, \theta_p)$ with respect to the input parameter θ . It measures the effect of the output when the input variable is perturbed one at a time around a nominal value. It serves as a first check, in most analysis, in screening parameters for identifiability. The

method evaluates elementary effects [36, 37, 38] with the i th parameter through the forward perturbation

$$g_i(\theta) = \frac{f(\theta_1, \theta_2, \dots, \theta_i + \Delta\theta_i, \dots, \theta_p) - f(\theta_1, \dots, \theta_p)}{\Delta\theta_i}, \quad i = 1(1)p$$

Morris [39] proposed two sensitivity measures, the mean (μ) and the standard deviation ($\tilde{\sigma}$) of the elementary effects. For non-monotonic models, μ may lead to a very small value due to cancellation effects. For this reason, Campolongo *et al.* [40] proposed the use of absolute values for evaluating the mean. In order to obtain a dimension-free sensitivity, we prefer the use of the sensitivity measure δ given in Brun *et al.* [41] as

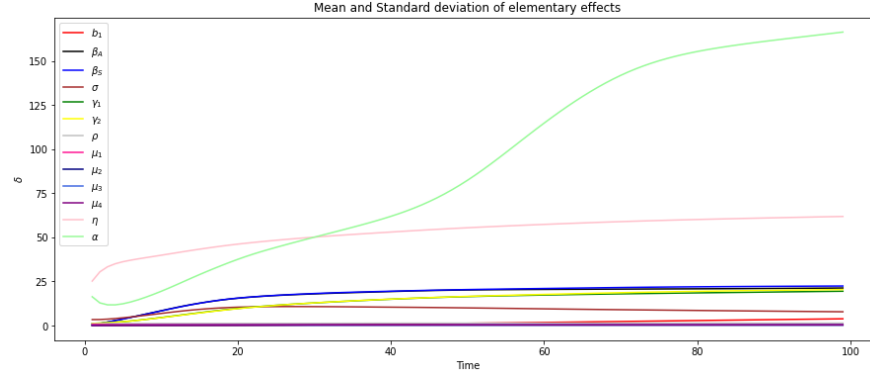
$$\delta_i = \sqrt{\frac{1}{N} \sum_{j=1}^N \tilde{g}_{ij}^2}, \quad i = 1(1)p, \text{ and } j = 1(1)N,$$

where N is the number of sample points and

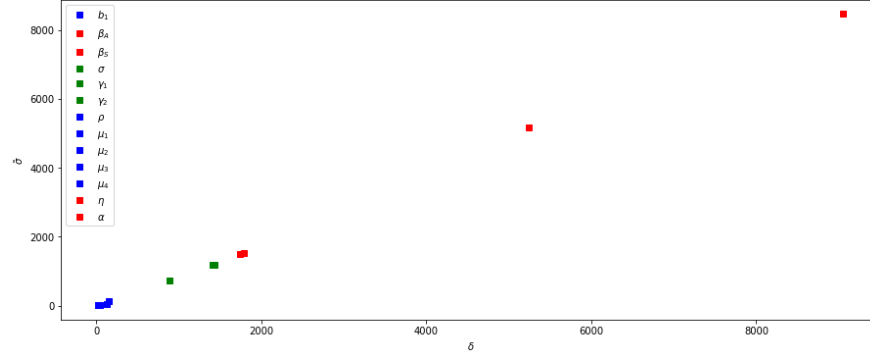
$$\tilde{g}_i(\theta) = \frac{f(\theta_1, \theta_2, \dots, \theta_i + \Delta\theta_i, \dots, \theta_p) - f(\theta_1, \dots, \theta_p)}{\Delta\theta_i} \frac{\theta_i}{f(\theta_1, \dots, \theta_p)}.$$

A common practice in the literature [42, 43, 38] is to plot the indices δ against $\tilde{\sigma}$, the standard deviation. We see from Fig. 2(a) that the fractional order α has the highest influence on the model output over time. The transmission rates for the symptomatic and asymptomatic populations and, the fractional parameter η are the next most influential parameters in the model. This is further corroborated by Fig. 2(b). The four parameters (α, β_S, β_A and η) denoted by red squares are the most important parameters, that is they have the largest δ and $\tilde{\sigma}$ values. The parameters ($b_1, \rho, \mu_1, \mu_2, \mu_3$ and μ_4) represented by the blue squares have the least influence on the model output and can be considered unimportant. The other parameters represented by the green squares have more influence than the parameters represented by the blue squares.

One major setback of the Morris screening test for sensitivity analysis is the consideration of each parameter individually and independently of the other parameters. In real applications, this is not true as parameters have collinearity and dependencies on one another.



(a) Sensitivity of the parameters over time



(b) Parameter Importance

Figure 2: Morris screening test

4.1.2. Sobol Analysis

The Sobol method is a variance-based sensitivity analysis method which unlike the Morris screening method takes into account the effect of the relationship between each parameters of the model. It uses the decomposition of variance to calculate Sobol's sensitivity indices: first and total order sensitivity measures. The basic idea of the Sobol's method is the decomposition of the model output function $y = f(\theta_1, \dots, \theta_p)$ into summands of increasing dimensionality, that is

$$V(y) = V_{1,\dots,p} + \sum_{i=1}^p V_i + \sum_{i=1}^p \sum_{j>1}^p V_{i,j} + \dots$$

where V_i is the partial variance of the contribution of the parameter θ_i and $V_{i,\dots,s}$ is the partial variances caused by the interaction of the parameters $(\theta_1, \dots, \theta_s)$ for $s \leq p$.

The first order sensitivity index measures the main effect of parameter θ_i on the model output; that is the partial contribution of θ_i to the variance $V(y)$. The

index [44, 45] is defined as

$$S_i = \frac{V_i}{V(y)}.$$

The larger this index, the more sensitive the parameter is to the model output [44, 45]. Using the law of total variances [45, 38], the index can also be expressed as

$$V(y) = V_{\theta_i}(E_{\theta_{\sim i}}(y|\theta_i)) + E_{\theta_i}(V_{\theta_{\sim i}}(y|\theta_i))$$

and

$$S_i = \frac{V_{\theta_i}(E_{\theta_{\sim i}}(y|\theta_i))}{V(y)}$$

where $V_{\theta_i}(E_{\theta_{\sim i}}(y|\theta_i))$ is the partial variance caused by θ_i and $E_{\theta_{\sim i}}(y|\theta_i)$ is the mean of the model output calculated by using all the values of the other parameters $\theta_{\sim i}$ (except θ_i) and $V(y)$ is the total variance.

The total sensitivity indices [46] measures the effects of parameter θ_i and the interaction with the other parameters. It is defined as

$$S_{T_i} = \frac{V_i + V_{i,j} + \dots + V_{i,j,\dots,p}}{V(y)}.$$

The total variance, $V(y)$, for this index is given as

$$V(y) = V_{\theta_{\sim i}}(E_{\theta_i}(y|\theta_{\sim i})) + E_{\theta_{\sim i}}(V_{\theta_i}(y|\theta_{\sim i}))$$

and

$$\begin{aligned} S_{T_i} &= \frac{E_{\theta_{\sim i}}(V_{\theta_i}(y|\theta_{\sim i}))}{V(y)} \\ &= \frac{V(y) - V_{\theta_{\sim i}}(E_{\theta_i}(y|\theta_{\sim i}))}{V(y)}. \end{aligned}$$

The mean and the variance can be evaluated using quasirandom sampling method [47, 38] and are given as

$$V_{\theta_i}(E_{\theta_{\sim i}}(y|\theta_i)) = \frac{1}{N} \sum_{j=1}^N f(\mathbf{B}_j) (f(\mathbf{A}_{\mathbf{B},j}^i) - f(\mathbf{A}_j)),$$

and

$$E_{\theta_{\sim i}}(V_{\theta_i}(y|\theta_{\sim i})) = \frac{1}{2N} \sum_{j=1}^N (f(\mathbf{A}_j) - f(\mathbf{A}_{\mathbf{B},j}^i))^2,$$

where \mathbf{A} and \mathbf{B} are two independent parameter sample matrices of dimensions $N \times p$. We shall use the python SALib package [48] to compute the first and total order variance indices. Fig. (3) shows that the fractional order β_S has the highest interaction with the other parameters. These results are consistent with the results in the Morris screening test as important parameters of the test show high interaction with the other parameters.

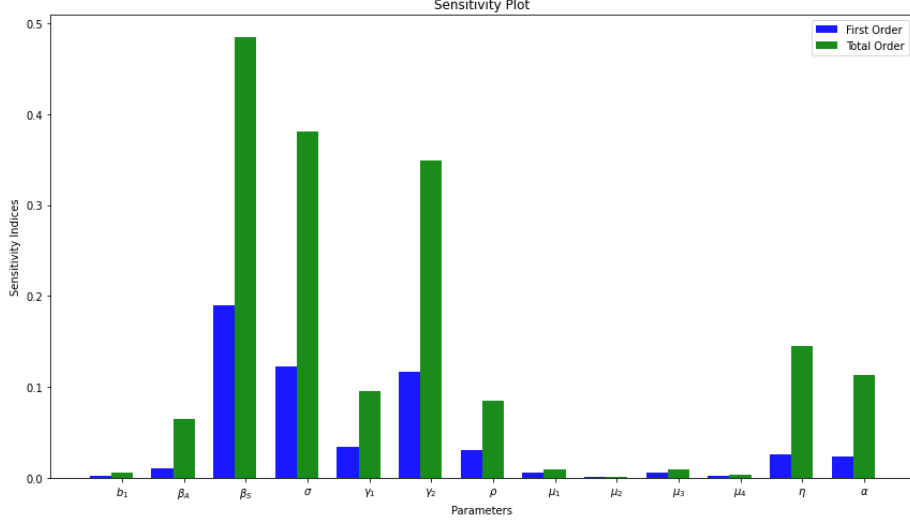


Figure 3: Sobol Sensitivity Indices

4.2. Parameter Identifiability

The concept of identifiability is dependent on sensitivity. It entails the selection of the subset of parameters of a model having little or no collinearity and uncertainty, and which can be identified uniquely from a given set of observed data or measurements. In other words, it answers the question "Can the available data be described by the model and the selected subset of parameters?". There are several techniques or tests for parameter identifiability. Most of the tests are based on the Fisher information matrix (FIM) $F = \chi^T \chi$ where $\chi = \partial y / \partial \theta$ for a model output function y . Cobelli and Di Stefano [49] showed that a sufficient condition for identifiability is the non-singularity of FIM. Burth *et al.* [50] proposed an iterative estimation process which implements a reduced-order estimation by finding parameters whose axis lie closest to the direction of FIM. The associated parameter values are then fixed at prior estimates during the iterated process. Brun *et al.* [41] studied parameter identifiability using two indices; a parameter importance ranking index δ and a collinearity index γ_K which depends on the smallest eigenvalues of submatrices of $\chi^T \chi$ corresponding to the parameter subset K . Cintr3n-Arias *et al.* [51] explained the need for a good parameter subset for identifiability to satisfy the full rank test. They further introduced two indices; the selection score and the condition number of $\chi^T \chi$. The smaller these indices the lesser the collinearity and uncertainty in the parameter values of the subset. Finally, they used the coefficient of variation index to examine the effect of parameters in the parameter subset. In this work, we shall use the test proposed by Cintr3n-Arias *et al.* in identifying the parameters. The algorithm can be summarized in the following steps

Algorithm 1 Algorithm for Parameter subset Selection [51]

- 1: Perform a combinatorial search for all possible parameter subsets. Let

$$S_p = \{\theta = (\lambda_1, \lambda_2, \dots, \lambda_p) \in \mathbb{R}^p \mid \lambda_k \in \mathcal{I} \text{ and } \lambda_k \neq \lambda_m \forall k, m = 1, \dots, p\},$$

where $\mathcal{I} = \{b_1, \beta_A, \beta_S, \sigma, \gamma_1, \gamma_2, \rho, \mu_1, \mu_2, \mu_3, \mu_4, \eta, \alpha\}$.

- 2: Select parameter subsets that pass the full rank test; that is

$$\Theta_p = \{\theta \mid \theta \in S_p \subset \mathbb{R}^p, \text{Rank}(\chi(\theta)) = p\}.$$

- 3: For each $\theta \in \Theta_p$, calculate the parameter selection score $\zeta(\theta) = |\vartheta(\theta)|$ where

$$\vartheta = \frac{\sqrt{\Sigma(\theta)_{ii}}}{\theta_i}, \quad i = 1, \dots, p,$$

and $\Sigma(\theta) = \sigma_0^2 [\chi^T(\theta)\chi(\theta)]^{-1} \in \mathbb{R}^p$.

- 4: Calculate the condition number $\kappa(\chi(\theta))$ for each parameter subset $\theta \in \Theta_p$. The smaller the values of $\kappa(\chi(\theta))$ and $\vartheta(\theta)$, the lower the uncertainty possibilities in the estimate.
-

To discuss the results in this section, we shall use the state of Tennessee as a case study to understand parameter identifiability. Furthermore, we used the following values obtained using a random search algorithm as the nominal parameter set θ_0 for the model:

$$\begin{aligned} b_1 &= 8.0316\text{e-}07, \quad \beta_A = 1.0000\text{e-}10, \quad \beta_S = 1.2312\text{e+}00, \quad \sigma = 9.9618\text{e-}01, \\ \gamma_1 &= 2.6628\text{e-}02, \quad \gamma_2 = 1.0000\text{e+}00, \quad \rho = 6.1740\text{e-}03, \quad \mu_1 = 3.3491\text{e-}03, \\ \mu_2 &= 1.0000\text{e-}10, \quad \mu_3 = 3.0859\text{e-}04, \quad \mu_4 = 2.1222\text{e-}05, \quad \eta = 1.5683\text{e-}01, \\ \alpha &= 1.0000\text{e+}00 \end{aligned}$$

and the nominal error variance $\sigma_0 = 10$. We further divide the parameters into three groups according to their importance rankings discussed in the previous section:

$$\begin{aligned} S_1 &= (\beta_A, \beta_S, \eta, \alpha), \\ S_2 &= (\sigma, \gamma_1, \gamma_2), \\ S_3 &= (b_1, \rho, \mu_1, \mu_2, \mu_3, \mu_4), \end{aligned}$$

where S_1 and S_3 are the most and least influential parameter sets, respectively, while S_2 contains more influential parameters than S_3 . We display some selections of the parameter subsets of size p in Table 1 where we have chosen the subsets with the smallest score values. The entries in Table 1 are ordered with respect to the selection score $\vartheta(\theta)$ for each subset of same cardinality. A high selection score and condition number for a parameter subset indicates substantial collinearity and linear dependence, and thus is poorly identifiable even if

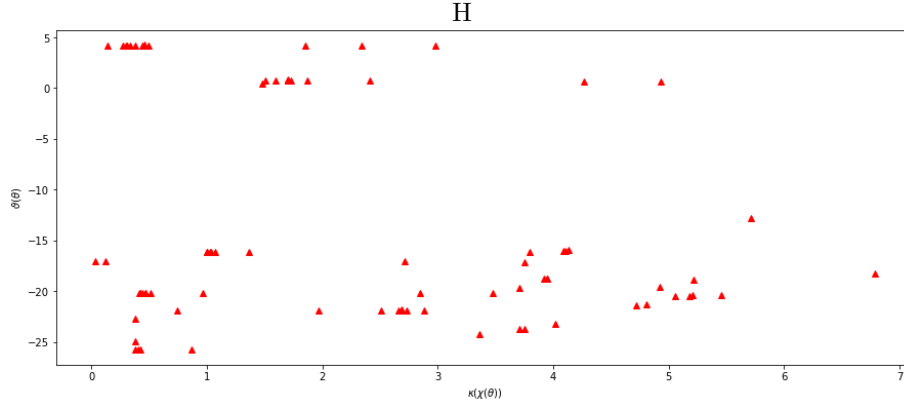


Figure 4: The condition number $\kappa(\chi(\theta))$ against the parameter selection scores $\vartheta(\theta)$ of the $N \times p$ sensitivity matrices for all parameter subsets $\theta = \Theta_p$ with $p = 2$. Logarithmic scales are used on both axis

the parameter subsets contains S_1 , that is contains the set of most influential parameters. We observe that most of the selections in Table 1 contains at least one element in each of the groups listed above. This shows that while parameter importance ranking is crucial in identifying parameters that drives the dynamics of a model, it does not have substantial effect in identifiability. Identifiability depends on proper selection of subsets including parameters in each of the three groups above that describes the measurement or data.

To have an idea of the variations of the condition number and the selection score, we give a plot of these values for $p = 2$ in fig. 4 (with logarithmic scales). Good parameter combination in fig. 4 corresponds to values in the lower left corner of the figure where the values, $\vartheta(\theta)$ and $\kappa(\chi(\theta))$, are relatively small.

p	Parameter Subsets	$\kappa(\chi(\theta))$	$\vartheta(\theta)$
13	$(b_1, \beta_A, \beta_S, \sigma, \gamma_1, \gamma_2, \rho, \mu_1, \mu_2, \mu_3, \mu_4, \eta, \alpha)$	9.530e+03	8.481e+01
12	$(b_1, \beta_A, \beta_S, \sigma, \gamma_1, \gamma_2, \rho, \mu_1, \mu_3, \mu_4, \eta, \alpha)$	9.513e+03	6.147e+00
11	$(b_1, \beta_S, \sigma, \gamma_1, \gamma_2, \rho, \mu_1, \mu_3, \mu_4, \eta, \alpha)$	4.814e+03	2.479e-04
10	$(b_1, \beta_S, \sigma, \gamma_1, \gamma_2, \rho, \mu_1, \mu_4, \eta, \alpha)$	3.696e+03	3.852e-07
	$(b_1, \beta_S, \sigma, \gamma_1, \gamma_2, \rho, \mu_3, \mu_4, \eta, \alpha)$	3.685e+03	4.143e-06
9	$(\beta_S, \sigma, \gamma_1, \gamma_2, \rho, \mu_1, \mu_4, \eta, \alpha)$	3.411e+03	2.766e-07
	$(b_1, \beta_S, \sigma, \gamma_1, \gamma_2, \rho, \mu_4, \eta, \alpha)$	3.311e+03	2.824e-07
7	$(\beta_S, \gamma_1, \gamma_2, \rho, \mu_4, \eta, \alpha)$	2.718e+03	5.344e-08
	$(\beta_S, \gamma_1, \gamma_2, \rho, \mu_1, \eta, \alpha)$	2.947e+03	5.388e-08
5	$(\gamma_1, \gamma_2, \rho, \mu_4, \alpha)$	6.171e+01	2.006e-09
	$(\beta_S, \gamma_1, \rho, \mu_4, \alpha)$	6.389e+01	2.006e-09
	$(\gamma_1, \rho, \mu_4, \eta, \alpha)$	6.989e+01	2.010e-09
4	$(\gamma_1, \rho, \eta, \alpha)$	6.258e+01	3.458e-10
	$(\gamma_1, \gamma_2, \rho, \alpha)$	5.289e+01	3.491e-10
	$(\beta_S, \gamma_1, \rho, \alpha)$	5.349e+01	3.496e-10
3	(γ_2, ρ, α)	5.140e+01	5.431e-11
	(β_S, ρ, α)	5.203e+01	5.850e-11
	(ρ, η, α)	6.224e+01	9.109e-11

Table 1: Selection scores and condition numbers for some selected parameter subsets

To further analyze the parameter identifiability of the model, we consider the parameters subsets:

$$\begin{aligned}
\theta_1 &= (b_1, \beta_A, \beta_S, \sigma, \gamma_1, \gamma_2, \rho, \mu_1, \mu_2, \mu_3, \mu_4, \eta, \alpha), \\
\theta_2 &= (b_1, \beta_S, \sigma, \gamma_1, \gamma_2, \rho, \mu_1, \mu_3, \mu_4, \eta, \alpha), \\
\theta_3 &= (\beta_S, \sigma, \gamma_1, \gamma_2, \rho, \mu_1, \mu_4, \eta, \alpha), \\
\theta_4 &= (\beta_S, \gamma_1, \gamma_2, \rho, \mu_4, \eta, \alpha), \\
\theta_5 &= (\gamma_1, \gamma_2, \rho, \mu_4, \alpha), \\
\theta_6 &= (\gamma_1, \gamma_2, \rho, \alpha), \\
\theta_7 &= (\gamma_2, \rho, \alpha)
\end{aligned}$$

such that $\theta_{i+1} \subset \theta_i$, $i = 1, \dots, 6$. The choice of these parameter subsets are due to their relative small condition numbers and selection scores. In other to create synthetic data, we assume the nominal parameter subsets and error variance (given at the beginning of this section) to be the true parameter vectors and true variance. Furthermore, we add random noise to the model output as follows:

$$Y_j = z(t_j, \theta_0) + \sigma_0 \mathcal{N}(0, 1), \quad j = 1, \dots, N.$$

We solve seven inverse problems for each of the parameter subsets θ_i , $i = 1, \dots, 7$. We analyze the result using the coefficient of variation and standard error [51] given as

$$SE_j(\tilde{\theta}) = \sqrt{\tilde{\Sigma}_{j,j}}, \quad j = 1, \dots, p$$

$\tilde{\theta}$	AIC	BIC
θ_1	164.80	198.67
θ_2	163.39	192.05
θ_3	150.84	174.28
θ_4	144.85	163.09
θ_5	142.63	155.68
θ_6	140.80	151.22
θ_7	141.68	149.50

Table 2: AIC and BIC metrics to estimate the quality of the model with different parameter sets.

and

$$v_j(\tilde{\theta}) = \frac{SE_j(\tilde{\theta})}{\tilde{\theta}_j}, \quad j = 1, \dots, p,$$

where $\tilde{\Sigma}_{j,j} = \tilde{\sigma}_0^2 \left[\chi(\tilde{\theta})^T \chi(\tilde{\theta}) \right]^{-1}$ and $\tilde{\sigma}_0^2 = \frac{1}{n-p} |Y - z(\tilde{\theta})|$.

From Table 6, it is seen that the parameters $(\mu_2, \mu_3) \subset \theta_1$ have standard errors that is approximately 20 times their estimates. This shows substantial uncertainty in these parameter values and any parameter subset containing these parameters may result in illogical parameter estimation from observations. The standard errors of $\beta_S, \gamma_1, \rho, \mu_3, \mu_4, \eta, \alpha$ in θ_2 show improvements and implies lower linear dependence and collinearity for parameters in θ_2 than those in θ_1 . Thus, a substantial improvement in uncertainty quantification is seen from θ_1 to θ_2 . Further improvements are observed for each of the other parameter subsets as more parameters are removed. For instance, with the removal of β_S and η in θ_4 , it seen that the standard error for γ_1 and γ_2 dropped from 4% and 1% to approximately 0.07% and 0.003%, respectively, of their estimates. Other improvements in θ_5 include α where the standard error is reduced to at least one-tenth of its standard error in θ_4 . We note that there is no substantial gain in the removal of μ_4 from θ_5 and γ_1 in θ_6 as seen in Table ??.

Parameter identifiability might be misleading without the investigation of the residual of the model [51]. The Akaike Information Criterion (AIC) and Bayesian Information Criterion (BIC) indices make use of residuals to determine the quality of models in the presence of a given set of data. Table 2 shows the AIC and BIC estimates for each parameter set θ_i , $i = 1, \dots, 7$. It is seen that the best improvements occur from θ_i to θ_{i+1} for $i = 2, 3$. Thus, the best case scenario of uncertainty quantification obtained for this analysis is that of θ_4 .

Finally, we present results in Table 3 obtained from solving the inverse problem for θ_4 using the data given in [52]. The remaining parameters are fixed using the nominal parameters above and T^* is the number of days used in the simulation

Parameters	Estimates	Standard Errors	Coefficients of Variation
β_S	9.9792e-01	1.8476e-01	1.8514e-01
γ_1	7.2723e-02	6.2483e-03	8.5918e-02
γ_2	2.9536e-01	2.2578e-02	7.6443e-02
ρ	1.9201e-02	4.9837e-04	2.5956e-02
μ_4	2.5413e-04	2.7412e-04	1.0786e+00
η	6.7561e-01	4.2262e-02	6.2554e-02
α	9.8887e-01	2.9311e-02	2.9641e-02

Table 3: Final parameter estimates from the data given in [52] with $T^* = 100$

5. Results and Discussions

Seven inverse problems for California, Florida, Georgia, Maryland, Texas, Washington and Wisconsin were solved to estimate the full parameter sets of the model. As seen in fig. 5, the fits are reasonably good even for states like Tennessee and Wisconsin whose current infected population begins to flatten. Table 7 (see Appendix) shows the fit parameter sets for each of the states with T^* being the number of days used in the simulation. We see that the contact rates β_A^α and β_S^α for the asymptomatic and symptomatic population lies within $0.5\text{--}1.5\text{ days}^{-1}$, a range suggested by Li *et al.* [53], Read *et al.* [54], Shen *et al.* [55], Eikenberry *et al.* [56]. The incubation period $1/\sigma^\alpha$ is seen to be relatively small, around 1–2 days. The average length of active infection $1/\gamma_1^\alpha$ and $1/\gamma_2^\alpha$ of the asymptomatic and symptomatic population, respectively, is seen to be around 1–27 days which is in line with suggested range of days in the literature [57, 58]. The recovery rate via hospitalization is seen to be very small for California, Florida, Georgia and Washington where the data records little or no recovery at all for infected patients. The death rates $\mu_1^\alpha, \mu_2^\alpha, \mu_3^\alpha, \mu_4^\alpha$ from the exposed, asymptomatic infected, symptomatic infected and hospitalized compartments are seen to be relatively small ranging from $0\text{--}0.01\text{ day}^{-1}$. With a μ_4^α value of around 0, Florida and Georgia has no death from the hospitalized compartments. This is reasonable since ρ^α is also practically 0 indicating no recovery for this states as seen in the data (not shown here).

Table 4 shows the basic reproduction number R_0 values computed for our model using (3) and the parameters listed in Table 7. The epidemic is expected to continue indefinitely if $R_0 > 1$ as predicted for all states. This suggest that stricter measures such as the use of masks in public places, social distancing, contact tracing and even longer stay-at-home orders need to be enforced in order to eradicate the epidemic. Fig. 5 shows plot of the infected (asymptomatic plus symptomatic), recovered and deaths. We see that shape of most curves are similar except for Wisconsin and Tennessee where the infected population begin to flatten over time. In particular, spikes of the curves in fig. 5 begin around late March or early April 2020 and continues to rise.

Table 5 shows a computational comparison of the proposed model and the integer-order counterpart using the sum squared errors (SSE) obtained for the

States	R_0
California	1.0837
Florida	1.1340
Georgia	1.1096
Maryland	1.2501
Texas	1.2367
Tennessee	1.0343
Washington	1.0964
Wisconsin	1.0754

Table 4: The basic reproduction number R_0 values for the selected states.

States	Integer-order model	Fractional-order model
California	8.323e+09	2.898e+09
Florida	3.688e+09	2.544e+09
Georgia	2.995e+09	7.464e+08
Maryland	6.277e+08	6.551e+08
Tennessee	3.308e+08	1.054e+08
Texas	5.473e+09	2.712e+09
Washington	8.780e+08	3.103e+08
Wisconsin	7.404e+08	3.165e+08

Table 5: Comparison of sum squared errors (SSE) of the proposed model to the integer-order counterpart

infected, recovered and dead populations. As seen in the table, the fractional-order model shows superiority over the integer-order model in fitting the COVID-19 pandemic. In fig. 6, we show the cumulative infected and hospitalized population. This plot also shows that while the infected population flatten over time for states like California, Florida, Maryland, Tennessee, Texas and Wisconsin, it increases for Georgia and Washington. If drastic measures are not taken, the model suggest that many will be infected, at some point, before the end of 2021 in these states.

6. Conclusions

A fractional-order compartmental model is proposed to study the spread and dynamics of the COVID-19 pandemic. We studied the properties of the model and discussed the parameters of the model in the context of sensitivity and identifiability. We solve several inverse problems to estimate the fit parameters of the model using data from John Hopkins University [59] for some selected states in the US. The basic reproduction number R_0 of the model was computed and shows that the states considered have R_0 values slightly greater than the critical value of one. The model suggests that stricter or aggressive measures need be enforced in order to slow the spread of the virus.

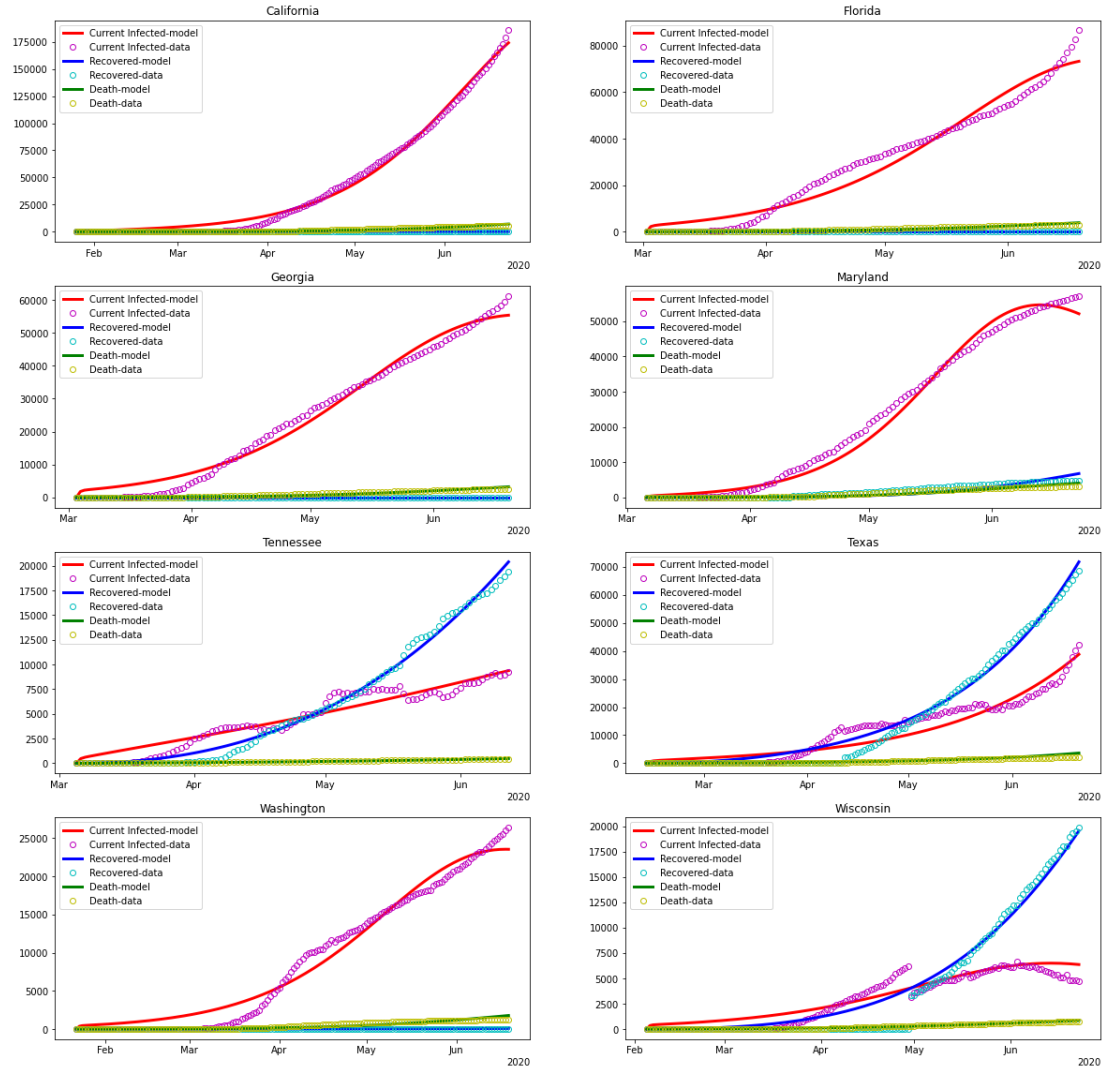


Figure 5: Model fits of the compartmental model to infected, recovered and deaths.

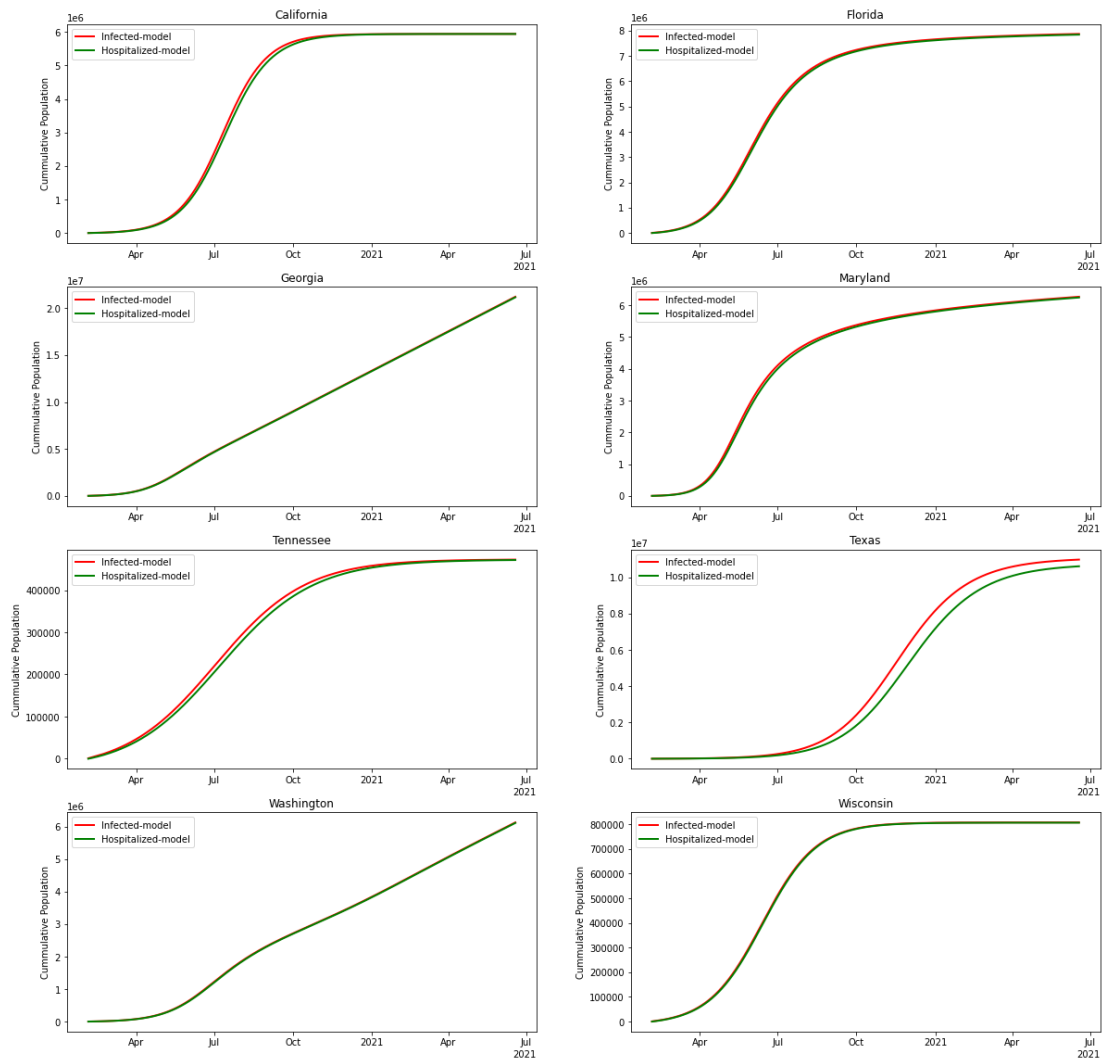


Figure 6: Model prediction for cumulative infected and hospitalized populations

Acknowledgement

The authors are grateful to the anonymous referees for their constructive criticisms and insightful suggestions in making the manuscript a better one.

References

- [1] E. Di Giuseppe, M. Moroni, M. Caputo, Flux in porous media with memory: models and experiments, *Transport in Porous Media* 83 (3) (2010) 479–500.
- [2] D. Baleanu, K. Diethelm, E. Scalas, J. J. Trujillo, *Fractional Calculus: models and numerical methods*, Vol. 5, World Scientific, 2016.
- [3] I. Podlubny, *Fractional differential equations*, *Mathematics in Science and Engineering* 198, Academic Press, 1999 (1999).
- [4] M. Caputo, F. Mainardi, A new dissipation model based on memory mechanism, *Pure and Applied Geophysics* 91 (1) (1971) 134–147.
- [5] S. Fomin, V. Chugunov, T. Hashida, Mathematical modeling of anomalous diffusion in porous media, *Fractional Differential Calculus* 1 (1) (2011) 1–28.
- [6] R. Metzler, J. Klafter, The random walk’s guide to anomalous diffusion: a fractional dynamics approach, *Physics reports* 339 (1) (2000) 1–77.
- [7] A. Cloot, J. Botha, A generalised groundwater flow equation using the concept of non-integer order derivatives, *Water SA* 32 (1) (2006) 1–7.
- [8] G. Iaffaldano, M. Caputo, S. Martino, Experimental and theoretical memory diffusion of water in sand, *Hydrology and Earth System Sciences Discussions* 2 (4) (2005) 1329–1357.
- [9] I. Podlubny, *Fractional-order systems and fractional-order controllers*, *Institute of Experimental Physics, Slovak Academy of Sciences, Kosice* 12 (3) (1994) 1–18.
- [10] R. L. Magin, Fractional calculus models of complex dynamics in biological tissues, *Computers & Mathematics with Applications* 59 (5) (2010) 1586 – 1593, *fractional Differentiation and Its Applications*.
- [11] J. T. Machado, A. C. Costa, M. D. Quelhas, Fractional dynamics in DNA, *Communications in Nonlinear Science and Numerical Simulation* 16 (8) (2011) 2963 – 2969.
- [12] K. Shah, M. A. Alqudah, F. Jarad, T. Abdeljawad, Semi-analytical study of Pine Wilt disease model with convex rate under Caputo–Fabrizio fractional order derivative, *Chaos, Solitons & Fractals* 135 (2020) 109754.

- [13] C. Ionescu, A. Lopes, D. Copot, J. Machado, J. Bates, The role of fractional calculus in modeling biological phenomena: A review, *Communications in Nonlinear Science and Numerical Simulation* 51 (2017) 141 – 159.
- [14] D. Baleanu, A. Jajarmi, S. S. Sajjadi, J. H. Asad, The fractional features of a harmonic oscillator with position-dependent mass, *Communications in Theoretical Physics* 72 (5) (2020) 055002.
- [15] K. Diethelm, A fractional calculus based model for the simulation of an outbreak of Dengue fever, *Nonlinear Dynamics* 71 (613–619) (2013).
- [16] M. R. Islam, A. Peace, D. Medina, T. Oraby, Integer Versus Fractional Order SEIR Deterministic and Stochastic Models of Measles, *Int J. Environ Res. Public Health* 17 (6) (2020).
- [17] D. Baleanu, A. Jajarmi, H. Mohammadi, S. Rezapour, A new study on the mathematical modelling of human liver with Caputo–Fabrizio fractional derivative, *Chaos, Solitons & Fractals* 134 (2020) 109705.
- [18] D. Sierociuk, T. Skovranek, M. Macias, I. Podlubny, I. Petras, A. Dzielinski, P. Ziubinski, Diffusion process modeling by using fractional-order models, *Applied Mathematics and Computation* 257 (2015) 2 – 11, Recent Advances in Fractional Differential Equations.
- [19] R. Almeida, Analysis of a fractional SEIR model with treatment, *Applied Mathematics Letters* 84 (2018) 56 – 62.
- [20] New York Times, <https://www.nytimes.com/2020/05/15/us/coronavirus-first-case-snohomish-antibodies.html>.
- [21] CNN News, <https://www.cnn.com/2020/04/20/us/states-that-require-masks-trnd/index.html>.
- [22] Z. Lu, Y. Yu, Y. Chen, G. Ren, C. Xu, S. Wang, Z. Yin, A fractional-order SEIHDR model for COVID-19 with inter-city networked coupling effects (2020). [arXiv:2004.12308](https://arxiv.org/abs/2004.12308).
- [23] Z. Liu, P. Magal, O. Seydi, G. Webb, Understanding Unreported Cases in the COVID-19 Epidemic Outbreak in Wuhan, China, and the Importance of Major Public Health Interventions, *Biology* 9 (50) (2020).
- [24] G. Giordano, F. Blanchini, R. Bruno, P. Colaneri, A. D. Filippo, A. D. Matteo, M. Colaneri, Modelling the COVID-19 epidemic and implementation of population-wide interventions in Italy, *Nature Medicine* 26 (2020) 855–860.
- [25] L. Stella, A. P. Martínez, D. Bauso, P. Colaneri, The Role of Asymptomatic Individuals in the COVID-19 Pandemic via Complex Networks (2020). [arXiv:2009.03649](https://arxiv.org/abs/2009.03649).

- [26] J. T. Wu, K. Leung, G. M. Leung, Nowcasting and forecasting the potential domestic and international spread of the 2019-nCoV outbreak originating in Wuhan, China: a modelling study, *The Lancet* 395 (10225) (2020) 689 – 697.
- [27] S. Zhao, H. Chen, Modeling the epidemic dynamics and control of COVID-19 outbreak in China, *Quantitative Biology* 8 (1) (2020) 11.
- [28] Y. Zhang, X. Yu, H. Sun, G. R. Tick, W. Wei, B. Jin, Applicability of time fractional derivative models for simulating the dynamics and mitigation scenarios of COVID-19, *Chaos, Solitons & Fractals* 138 (2020) 109959.
- [29] N. H. Tuan, H. Mohammadi, S. Rezapour, A mathematical model for covid-19 transmission by using the caputo fractional derivative, *Chaos, Solitons & Fractals* 140 (2020) 110107.
- [30] M. Bahloul, A. Chahid, T.-M. Laleg-Kirati, Fractional-order SEIQRDP Model for Simulating the Dynamics of COVID-19 Epidemic, *IEEE Open Journal of Engineering in Medicine and Biology* 1 (2020) 249–256.
- [31] M. Caputo, Linear model of dissipation whose q is almost frequency independent. ii, *Geophysical Journal International* 13 (5) (1967) 529–539.
- [32] Y. Li, Y. Chen, I. Podlubny, Mittag-leffler stability of fractional order nonlinear dynamic systems, *Automatica* 45 (8) (2009) 1965 – 1969.
- [33] O. Diekmann, J. Heesterbeek, J. Metz, On the definition and the computation of the basic reproduction ratio R_0 in models for infectious diseases in heterogeneous populations, *Journal of Mathematical Biology* 28 (1990) 365–382.
- [34] P. van den Driessche, J. Watmough, Reproduction numbers and sub-threshold endemic equilibria for compartmental models of disease transmission, *Mathematical Biosciences* 180 (1) (2002) 29 – 48.
- [35] O. Diekmann, J. A. P. Heesterbeek, M. G. Roberts, The construction of next-generation matrices for compartmental epidemic models, *Journal of Royal Society Interface* (2009) 7873–885.
- [36] A. Saltelli, S. Tarantola, F. Campolongo, Sensitivity analysis as an ingredient of modeling, *Statistical Science* 15 (4) (2000) 377–395.
- [37] A. Saltelli, S. Tarantola, F. Campolongo, M. Ratto, Sensitivity analysis in practice: a guide to assessing scientific models, John Willy & Sons, Ltd, 2004.
- [38] M. Ye, M. Hill, Chapter 10 - Global Sensitivity Analysis for Uncertain Parameters, Models, and Scenarios, in: G. P. Petropoulos, P. K. Srivastava (Eds.), *Sensitivity Analysis in Earth Observation Modelling*, Elsevier, 2017, pp. 177 – 210.

- [39] M. D. Morris, Factorial sampling plans for preliminary computational experiments, *Technometrics* 33 (2) (1991) 161–174.
- [40] F. Campolongo, J. Cariboni, A. Saltelli, An effective screening design for sensitivity analysis of large models, *Environmental Modelling & Software* 22 (10) (2007) 1509 – 1518, modelling, computer-assisted simulations, and mapping of dangerous phenomena for hazard assessment.
- [41] R. Brun, P. Reichert, H. R. Künsch, Practical identifiability analysis of large environmental simulation models, *Water Resources Research* 37 (4) (2001) 1015–1030.
- [42] K. Pohlmann, M. Ye, D. Reeves, M. Zavarin, D. Decker, J. Chapman, Modeling of Groundwater Flow and Radionuclide Transport at the Climax Mine sub-CAU, Nevada Test Site (DOE/NV-26383-06) United States (Sep 2007).
- [43] Y. Ming, W. Liying, K. Pohlmann, J. Chapman, Evaluating groundwater interbasin flow using multiple models and multiple types of data, *Groundwater* 54 (6) (2016) 805–817.
- [44] I. Sobol, Sensitivity analysis for nonlinear mathematical models, *Mathematical Models and Computer Experiment* 1 (4) (1993) 407–414.
- [45] I. M. Sobol, Global sensitivity indices for nonlinear mathematical models and their Monte Carlo estimates, *Mathematics and Computers in Simulation* 55 (1) (2001) 271 – 280, the Second IMACS Seminar on Monte Carlo Methods.
- [46] T. Homma, A. Saltelli, Importance measures in global sensitivity analysis of nonlinear models, *Reliability Engineering & System Safety* 52 (1) (1996) 1 – 17.
- [47] A. Saltelli, P. Annoni, I. Azzini, F. Campolongo, M. Ratto, S. Tarantola, Variance based sensitivity analysis of model output. design and estimator for the total sensitivity index, *Computer Physics Communications* 181 (2) (2010) 259–270.
- [48] Python SALib Package, <https://salib.readthedocs.io/en/latest/>.
- [49] C. Cobelli, J. J. DiStefano, Parameter and structural identifiability concepts and ambiguities: a critical review and analysis, *American Journal of Physiology-Regulatory, Integrative and Comparative Physiology* 239 (1) (1980) R7–R24.
- [50] M. Burth, G. C. Verghese, M. Velez-Reyes, Subset selection for improved parameter estimation in on-line identification of a synchronous generator, *IEEE Transactions on Power Systems* 14 (1) (1999) 218–225.

- [51] A. Cintrón-Arias, H. T. Banks, A. Capaldi, A. L. Lloyd, A sensitivity matrix based methodology for inverse problem formulation, *Journal of Inverse and Ill-posed Problems* 17 (6) (2009) 545 – 564.
- [52] Tennessee Department of Health, <https://www.tn.gov/health/cedep/ncov/data/downloadable-datasets.html>.
- [53] R. Li, S. Pei, B. Chen, Y. Song, T. Zhang, W. Yang, J. Shaman, Substantial undocumented infection facilitates the rapid dissemination of novel coronavirus (SARS-CoV-2), *Science* 368 (6490) (2020) 489–493.
- [54] J. M. Read, J. R. Bridgen, D. A. Cummings, A. Ho, C. P. Jewell, Novel coronavirus 2019-nCoV: early estimation of epidemiological parameters and epidemic predictions, *medRxiv* (2020).
- [55] M. Shen, Z. Peng, Y. Xiao, L. Zhang, Modelling the epidemic trend of the 2019 novel coronavirus outbreak in China, *bioRxiv* (2020).
- [56] S. E. Eikenberry, M. Mancuso, E. Iboi, T. Phan, K. Eikenberry, Y. Kuang, E. Kostelich, A. B. Gumel, To mask or not to mask: Modeling the potential for face mask use by the general public to curtail the COVID-19 pandemic, *Infectious Disease Modelling* 5 (2020) 293 – 308.
- [57] B. Tang, N. L. Bragazzi, Q. Li, S. Tang, Y. Xiao, J. Wu, An updated estimation of the risk of transmission of the novel coronavirus (2019-ncov), *Infectious Disease Modelling* 5 (2020) 248 – 255.
- [58] F. Zhou, T. Yu, R. Du, G. Fan, Y. Liu, Z. Liu, J. Xiang, Y. Wang, B. Song, X. Gu, L. Guan, Y. Wei, Clinical course and risk factors for mortality of adult inpatients with COVID-19 in Wuhan, China: a retrospective cohort study, *The Lancet* 395 (10229) (2020) 1054 – 1062.
- [59] Johns Hopkins University. https://github.com/CSSEGISandData/COVID-19/tree/master/csse_covid_19_data/csse_covid_19_daily_reports, 2020.
- [60] W. Lin, Global existence theory and chaos control of fractional differential equations, *Journal of Mathematical Analysis and Applications* 332 (1) (2007) 709 – 726.
- [61] United States Census Bureau. <https://www2.census.gov/programs-surveys/popest/datasets/2010-2019/national/totals>, 2020.
- [62] T. A. Biala, A. Q. M. Khaliq, Parallel Algorithms for nonlinear time-space fractional parabolic PDEs, *Journal of Computational Physics* 375 (2018) 135–154.

Appendices

Appendix A. Proof of Theorem 3.1.

Proof. By applying [60, Theorem 3.1], we obtain the existence of the solutions. To show the uniqueness and boundedness of solutions, it suffices to show, by [60, Remark 3.2] and Rademacher's theorem, that $F = (f_1, f_2, f_3, f_4, f_5, f_6)$ is locally Lipschitz continuous where

$$\begin{aligned} f_1 &= b_1^\alpha N - \frac{S}{N} (\beta_A^\alpha I_A + \beta_S^\alpha I_S) - b_1^\alpha S, \\ f_2 &= \frac{S}{N} (\beta_A^\alpha I_A + \beta_S^\alpha I_S) - (\sigma^\alpha + \mu_1^\alpha) E, \\ f_3 &= \eta \sigma^\alpha E - (\gamma_1^\alpha + \mu_2^\alpha) I_A, \\ f_4 &= (1 - \eta) \sigma^\alpha E - (\gamma_2^\alpha + \mu_3^\alpha) I_S, \\ f_5 &= \gamma_1^\alpha I_A + \gamma_2^\alpha I_S - (\rho^\alpha + \mu_4^\alpha) H, \\ f_6 &= \rho^\alpha H - b_1^\alpha R. \end{aligned}$$

Let $X = (S, E, I_A, I_S, H, R)$, $\tilde{X} = (\tilde{S}, \tilde{E}, \tilde{I}_A, \tilde{I}_S, \tilde{H}, \tilde{R})$ and $\|\cdot\|$ denote the L_2 norm, then

$$\begin{aligned} \|F(X) - F(\tilde{X})\| &\leq \|f_1(X) - f_1(\tilde{X})\| + \|f_2(X) - f_2(\tilde{X})\| \\ &\quad + \|f_3(X) - f_3(\tilde{X})\| + \|f_4(X) - f_4(\tilde{X})\| \\ &\quad + \|f_5(X) - f_5(\tilde{X})\| + \|f_6(X) - f_6(\tilde{X})\| \\ &\leq L \|X - \tilde{X}\|, \end{aligned}$$

where $L = \max L_i$ and $L_1 = b_1^\alpha(N + 1) + \beta_A^\alpha + \beta_S^\alpha$, $L_2 = \beta_A^\alpha + \beta_S^\alpha + \sigma^\alpha + \mu_1^\alpha$, $L_3 = \eta \sigma^\alpha + \gamma_1^\alpha + \mu_2^\alpha$, $L_4 = (1 - \eta) \sigma^\alpha + \gamma_2^\alpha + \mu_3^\alpha$, $L_5 = \gamma_1^\alpha + \gamma_2^\alpha + \rho^\alpha + \mu_4^\alpha$ and $L_6 = \rho^\alpha + b_1^\alpha$. Thus, F satisfies the local Lipschitz conditions with respect to X which proves the uniqueness and boundedness of solution to (2). Next we show the non-negativity of solutions. At first, we consider moving along the S -axis, that is $E(0) = I_A(0) = I_S(0) = H(0) = R(0) = 0$ and $0 < S(0) = S_0 \leq N$, then

$${}_0\mathcal{D}_t^\alpha S(t) = b_1^\alpha N - b_2^\alpha S$$

whose solution is given as

$$S(t) = S_0 E_{\alpha,1}(-b_1^\alpha t^\alpha) + b_1^\alpha N t^\alpha E_{\alpha,\alpha+1}(-b_1^\alpha t^\alpha) > 0$$

since $b_1^\alpha > 0$ and $t > 0$. In a similar manner, moving along each of the other respective axis (that is all initial conditions are zeros except for the axis being considered), it is easy to show that

$$\begin{aligned} E(t) &= E_{\alpha,1}(-(\sigma^\alpha + \mu_1^\alpha)t^\alpha) E_0 \geq 0 \\ I_A(t) &= E_{\alpha,1}(-(\gamma_1^\alpha + \mu_2^\alpha)t^\alpha) I_{A0} \geq 0 \\ I_S(t) &= E_{\alpha,1}(-(\gamma_2^\alpha + \mu_3^\alpha)t^\alpha) I_{S0} \geq 0 \\ H(t) &= E_{\alpha,1}(-(\rho^\alpha + \mu_4^\alpha)t^\alpha) H_0 \geq 0 \\ R(t) &= E_{\alpha,1}(-b_1^\alpha t^\alpha) R_0 \geq 0. \end{aligned}$$

Therefore, all axis are non-negative invariant. Now, if the solution of the system is positive in the $E - I_A - I_S - H - R$ plane, then let $S(t^*) = 0$, $E(t^*) > 0$, $I_A(t^*) > 0$, $I_S(t^*) > 0$, $H(t^*) > 0$ and $R(t^*) > 0$ for some t^* such that $S(t) < S(t^*)$. But

$${}_0\mathcal{D}_t^\alpha S|_{t=t^*} = b_1^\alpha N > 0$$

in this plane. Using the mean value theorem for Caputo-fractional derivative

$$S(t) - S(t^*) = \frac{1}{\Gamma(\alpha)} \mathcal{D}_t^\alpha(\tau)(t - t^*)^\alpha$$

for some $\tau \in [t^*, t)$, we see that $S(t) > S(t^*)$. This contradicts our previous statement. Similar arguments can be used for each of the remaining population variables. \square

Appendix B. Proof of Theorem 3.2

Proof. The Jacobian matrix evaluated at the DFE point is given as

$$J = \begin{bmatrix} -b_1^\alpha & 0 & -\beta_A^\alpha & -\beta_S^\alpha & 0 & 0 \\ 0 & -(\sigma^\alpha + \mu_1^\alpha) & \beta_A^\alpha & \beta_S^\alpha & 0 & 0 \\ 0 & \eta\sigma^\alpha & -(\gamma_1^\alpha + \mu_2^\alpha) & 0 & 0 & 0 \\ 0 & (1 - \eta)\sigma^\alpha & 0 & -(\gamma_2^\alpha + \mu_3^\alpha) & 0 & 0 \\ 0 & 0 & \gamma_1^\alpha & \gamma_2^\alpha & -(\rho^\alpha + \mu_4^\alpha) & 0 \\ 0 & 0 & 0 & 0 & \rho^\alpha & -b_1^\alpha \end{bmatrix}.$$

The eigenvalues of the Jacobian matrix are given as $\lambda_1 = \lambda_2 = -b_1^\alpha$, $\lambda_3 = -(\rho^\alpha + \mu_4^\alpha)$ and the roots of the equation $z^3 + Az^2 + Bz + C$, where

$$A = (\sigma^\alpha + \gamma_1^\alpha + \gamma_2^\alpha + \mu_1^\alpha + \mu_2^\alpha + \mu_3^\alpha),$$

$$B = -\sigma^\alpha(\eta\beta_A^\alpha + (1 - \eta)\beta_S^\alpha) + (\sigma^\alpha + \mu_1^\alpha)(\gamma_1^\alpha + \mu_2^\alpha) + (\sigma^\alpha + \mu_1^\alpha)(\gamma_2^\alpha + \mu_3^\alpha) + (\gamma_1^\alpha + \mu_2^\alpha)(\gamma_2^\alpha + \mu_3^\alpha),$$

$$C = -\sigma^\alpha(\eta(\gamma_2^\alpha + \mu_3^\alpha)\beta_A^\alpha + (1 - \eta)(\gamma_1^\alpha + \mu_2^\alpha)\beta_S^\alpha) + (\sigma^\alpha + \mu_1^\alpha)(\gamma_1^\alpha + \mu_2^\alpha)(\gamma_2^\alpha + \mu_3^\alpha).$$

To show stability, we apply the Routh-Hurwitz criterion. Clearly $A > 0$ and $C > 0$ if $R_0 < 1$. It is easy to show that $AB > C$ if $K < 1$ which completes the proof. \square

Appendix C. Proof of Theorem 3.3

Proof. The Jacobian matrix evaluated at the EE point is given as

$$J = \begin{bmatrix} -b_1^\alpha - b_1^\alpha \left(1 - \frac{1}{R_0}\right) & 0 & -\frac{\beta_A^\alpha}{R_0} & -\frac{\beta_S^\alpha}{R_0} & 0 & 0 \\ b_1^\alpha \left(1 - \frac{1}{R_0}\right) & -(\sigma^\alpha + \mu_1^\alpha) & \frac{\beta_A^\alpha}{R_0} & \frac{\beta_S^\alpha}{R_0} & 0 & 0 \\ 0 & \eta\sigma^\alpha & -(\gamma_1^\alpha + \mu_2^\alpha) & 0 & 0 & 0 \\ 0 & (1 - \eta)\sigma^\alpha & 0 & -(\gamma_2^\alpha + \mu_3^\alpha) & 0 & 0 \\ 0 & 0 & \gamma_1^\alpha & \gamma_2^\alpha & -(\rho^\alpha + \mu_4^\alpha) & 0 \\ 0 & 0 & 0 & 0 & \rho^\alpha & -b_1^\alpha \end{bmatrix}.$$

The eigenvalues of the Jacobian matrix are $\lambda_1 = -b_1^\alpha$, $\lambda_2 = -(\rho^\alpha + \mu_4^\alpha)$ and the roots of the equation $z^4 + A_1 z^3 + A_2 z^2 + A_3 z + A_4$. By Applying the Routh-Hurwitz criterion, the EE is stable if $A_1 > 0$, $A_4 > 0$ and $(A_1 A_2 - A_3) A_3 - A_1^2 A_4 \geq 0$. Clearly $A_1 > 0$ since $R_0 > 1$. Also, $A_4 > 0$ implies that

$$\begin{aligned} & b_1^{3\alpha} R_0^3 (2R_0 - 1) (\sigma^\alpha + \mu_1^\alpha) (\gamma_1^\alpha + \mu_2^\alpha) (\gamma_2^\alpha + \mu_3^\alpha) > \sigma^\alpha ((1 - \eta) \beta_S^\alpha (\gamma_1^\alpha + \mu_2^\alpha) + \eta \beta_A^\alpha (\gamma_2^\alpha + \mu_3^\alpha)) lpha(\gamma_2^\alpha + \mu_3^\alpha) \\ \Rightarrow & b_1^{3\alpha} R_0^3 (2R_0 - 1) > \frac{\sigma^\alpha b_1^\alpha ((1 - \eta) \beta_S^\alpha (\gamma_1^\alpha + \mu_2^\alpha) + \eta \beta_A^\alpha (\gamma_2^\alpha + \mu_3^\alpha))}{(\sigma^\alpha + \mu_1^\alpha) (\gamma_1^\alpha + \mu_2^\alpha) (\gamma_2^\alpha + \mu_3^\alpha)} \\ \Rightarrow & b_1^{3\alpha} R_0^3 (2R_0 - 1) > 1 \text{ which is true since } R_0 > 1 \quad \square \end{aligned}$$

Appendix D. Data Sets and Methods

Data for cumulative confirmed cases, recovered and deaths were obtained from the Tennessee Department of Health (TDH) and Johns Hopkins University (JHU) Center for Systems Science and Engineering which are made available to the public on TDH's website [52] and Github [59], respectively. The raw files are converted into Panda data frames and stored for ease of access. For the files obtained from [59], the data are sorted according to counties, so we aggregate the cases for each of the recorded counties to obtain the total number of cases in each day for the states. For the total number of population for each states, we used the data obtained from the US Census Bureau [61].

All numerical simulations were done in python using our numerical scheme [62] from which we obtain the solution of the proposed model at each time step as

1. Predictor:

$$\begin{aligned} S_p &= S_j + \frac{\tau^\alpha}{\Gamma(1 + \alpha)} F_1(t_j, S_j, E_j, I_{A,j}, I_{S,j}, H_j, R_j, D_j) + \tilde{H}_{1,j} \\ E_p &= E_j + \frac{\tau^\alpha}{\Gamma(1 + \alpha)} F_2(t_j, S_j, E_j, I_{A,j}, I_{S,j}, H_j, R_j, D_j) + \tilde{H}_{2,j} \\ I_{A,p} &= I_{A,j} + \frac{\tau^\alpha}{\Gamma(1 + \alpha)} F_3(t_j, S_j, E_j, I_{A,j}, I_{S,j}, H_j, R_j, D_j) + \tilde{H}_{3,j} \\ I_{S,p} &= I_{S,j} + \frac{\tau^\alpha}{\Gamma(1 + \alpha)} F_4(t_j, S_j, E_j, I_{A,j}, I_{S,j}, H_j, R_j, D_j) + \tilde{H}_{4,j} \\ H_p &= H_j + \frac{\tau^\alpha}{\Gamma(1 + \alpha)} F_5(t_j, S_j, E_j, I_{A,j}, I_{S,j}, H_j, R_j, D_j) + \tilde{H}_{5,j} \\ R_p &= R_j + \frac{\tau^\alpha}{\Gamma(1 + \alpha)} F_6(t_j, S_j, E_j, I_{A,j}, I_{S,j}, H_j, R_j, D_j) + \tilde{H}_{6,j} \\ D_p &= D_j + \frac{\tau^\alpha}{\Gamma(1 + \alpha)} F_7(t_j, S_j, E_j, I_{A,j}, I_{S,j}, H_j, R_j, D_j) + \tilde{H}_{7,j} \end{aligned}$$

2. Corrector:

$$\begin{aligned}
S_{j+1} &= S_j + \frac{\tau^\alpha}{\Gamma(2+\alpha)} \left(\alpha F_1(t_j, S_j, E_j, I_{A,j}, I_{S,j}, H_j, R_j, D_j) \right. \\
&\quad \left. + F_1(t_{j+1}, S_p, E_p, I_{A,p}, I_{S,p}, H_p, R_p, D_p) \right) + \tilde{H}_{1,j}, \\
E_{j+1} &= E_j + \frac{\tau^\alpha}{\Gamma(2+\alpha)} \left(\alpha F_2(t_j, S_j, E_j, I_{A,j}, I_{S,j}, H_j, R_j, D_j) \right. \\
&\quad \left. + F_2(t_{j+1}, S_p, E_p, I_{A,p}, I_{S,p}, H_p, R_p, D_p) \right) + \tilde{H}_{2,j}, \\
I_{A,j+1} &= I_{A,j} + \frac{\tau^\alpha}{\Gamma(2+\alpha)} \left(\alpha F_3(t_j, S_j, E_j, I_{A,j}, I_{S,j}, H_j, R_j, D_j) \right. \\
&\quad \left. + F_3(t_{j+1}, S_p, E_p, I_{A,p}, I_{S,p}, H_p, R_p, D_p) \right) + \tilde{H}_{3,j}, \\
I_{S,j+1} &= I_{S,j} + \frac{\tau^\alpha}{\Gamma(2+\alpha)} \left(\alpha F_4(t_j, S_j, E_j, I_{A,j}, I_{S,j}, H_j, R_j, D_j) \right. \\
&\quad \left. + F_4(t_{j+1}, S_p, E_p, I_{A,p}, I_{S,p}, H_p, R_p, D_p) \right) + \tilde{H}_{4,j}, \\
H_{j+1} &= H_j + \frac{\tau^\alpha}{\Gamma(2+\alpha)} \left(\alpha F_5(t_j, S_j, E_j, I_{A,j}, I_{S,j}, H_j, R_j, D_j) \right. \\
&\quad \left. + F_5(t_{j+1}, S_p, E_p, I_{A,p}, I_{S,p}, H_p, R_p, D_p) \right) + \tilde{H}_{5,j}, \\
R_{j+1} &= R_j + \frac{\tau^\alpha}{\Gamma(2+\alpha)} \left(\alpha F_6(t_j, S_j, E_j, I_{A,j}, I_{S,j}, H_j, R_j, D_j) \right. \\
&\quad \left. + F_6(t_{j+1}, S_p, E_p, I_{A,p}, I_{S,p}, H_p, R_p, D_p) \right) + \tilde{H}_{6,j}, \\
D_{j+1} &= D_j + \frac{\tau^\alpha}{\Gamma(2+\alpha)} \left(\alpha F_7(t_j, S_j, E_j, I_{A,j}, I_{S,j}, H_j, R_j, D_j) \right. \\
&\quad \left. + F_7(t_{j+1}, S_p, E_p, I_{A,p}, I_{S,p}, H_p, R_p, D_p) \right) + \tilde{H}_{7,j},
\end{aligned}$$

where

$$\begin{aligned}
F_1(t_j, S_j, E_j, I_{A,j}, I_{S,j}, H_j, R_j, D_j) &= b_1^\alpha N - \frac{S_j}{N} (\beta_A^\alpha I_{A,j} + \beta_S^\alpha I_{S,j}) - b_1^\alpha S_j, \\
F_2(t_j, S_j, E_j, I_{A,j}, I_{S,j}, H_j, R_j, D_j) &= \frac{S_j}{N} (\beta_A^\alpha I_{A,j} + \beta_S^\alpha I_{S,j}) - (\sigma^\alpha + \mu_1^\alpha) E_j, \\
F_3(t_j, S_j, E_j, I_{A,j}, I_{S,j}, H_j, R_j, D_j) &= \eta \sigma^\alpha E_j - (\gamma_1^\alpha + \mu_2^\alpha) I_{A,j}, \\
F_4(t_j, S_j, E_j, I_{A,j}, I_{S,j}, H_j, R_j, D_j) &= (1 - \eta) \sigma^\alpha E_j - (\gamma_2^\alpha + \mu_3^\alpha) I_{S,j}, \\
F_5(t_j, S_j, E_j, I_{A,j}, I_{S,j}, H_j, R_j, D_j) &= \gamma_1^\alpha I_{A,j} + \gamma_2^\alpha I_{S,j} - (\rho^\alpha + \mu_4^\alpha) H_j, \\
F_6(t_j, S_j, E_j, I_{A,j}, I_{S,j}, H_j, R_j, D_j) &= \rho^\alpha H_j - b_1^\alpha R_j, \\
F_7(t_j, S_j, E_j, I_{A,j}, I_{S,j}, H_j, R_j, D_j) &= \mu_1^\alpha E_j + \mu_2^\alpha I_{A,j} + \mu_3^\alpha I_{S,j} + \mu_4^\alpha H_j,
\end{aligned}$$

and

$$\begin{aligned}
\tilde{H}_{1,j} &= \frac{\tau^\alpha}{\Gamma(2+\alpha)} \sum_{l=0}^j a_{l,j} F_1(t_l, S_l, E_l, I_{A,l}, I_{S,l}, H_l, R_l, D_l), \\
\tilde{H}_{2,j} &= \frac{\tau^\alpha}{\Gamma(2+\alpha)} \sum_{l=0}^j a_{l,j} F_2(t_l, S_l, E_l, I_{A,l}, I_{S,l}, H_l, R_l, D_l), \\
\tilde{H}_{3,j} &= \frac{\tau^\alpha}{\Gamma(2+\alpha)} \sum_{l=0}^j a_{l,j} F_3(t_l, S_l, E_l, I_{A,l}, I_{S,l}, H_l, R_l, D_l), \\
\tilde{H}_{4,j} &= \frac{\tau^\alpha}{\Gamma(2+\alpha)} \sum_{l=0}^j a_{l,j} F_4(t_l, S_l, E_l, I_{A,l}, I_{S,l}, H_l, R_l, D_l), \\
\tilde{H}_{5,j} &= \frac{\tau^\alpha}{\Gamma(2+\alpha)} \sum_{l=0}^j a_{l,j} F_5(t_l, S_l, E_l, I_{A,l}, I_{S,l}, H_l, R_l, D_l), \\
\tilde{H}_{6,j} &= \frac{\tau^\alpha}{\Gamma(2+\alpha)} \sum_{l=0}^j a_{l,j} F_6(t_l, S_l, E_l, I_{A,l}, I_{S,l}, H_l, R_l, D_l), \\
\tilde{H}_{7,j} &= \frac{\tau^\alpha}{\Gamma(2+\alpha)} \sum_{l=0}^j a_{l,j} F_7(t_l, S_l, E_l, I_{A,l}, I_{S,l}, H_l, R_l, D_l)
\end{aligned}$$

are the memory terms of the respective population variables and

$$a_{l,j} = \frac{\tau^\gamma}{\Gamma(\gamma+2)} \begin{cases} -(j-\gamma)(j+1)^\gamma + j^\gamma(2j-\gamma-1) - (j-1)^{\gamma+1}, & l=0, \\ (j-l+2)^{\gamma+1} - 3(j-l+1)^{\gamma+1} + 3(j-l)^{\gamma+1} - (j-l-1)^{\gamma+1}, & 1 \leq l \leq j-1, \\ 2^{\gamma+1} - \gamma - 3, & l=j. \end{cases}$$

The fitted parameters were obtained by using python's `scipy.optimize.minimize` routine with the limited memory BFGS method. One main benefit of the routine is the use of bounds for fit parameters. This allows faster convergence of the algorithm and ensures obtaining meaningful fit parameters of the model. The parameters are constrained to lie between 0 and 1 except for the transmission rates that are allowed to lie between 0.5 and 1.5 as suggested in [53, 54, 55, 56]. In some cases like Florida and Georgia where the data shows little or no recovery of the infected population, we constrain the fit parameter to lie within 0 and 1e-10. Fits were made comparing the simulation results and the data obtained from [59] for the infected, recovered and deaths.

Appendix E. Tables

	b_1	β_A	β_S	σ	γ_1	γ_2	ρ	μ_1	μ_2	μ_3	μ_4	η	α
$\tilde{\theta}$	1.13e-4	2.60e-4	1.23e+0	9.96e-1	2.69e-2	1.00e+0	6.18e-3	3.32e-3	1.59e-5	3.05e-4	2.13e-5	1.57e-1	1.00e+0
E	3.16e-6	1.42e-4	5.74e-3	2.29e-3	7.39e-4	4.56e-3	1.01e-5	4.94e-3	7.37e-4	6.48e-3	5.52e-5	9.47e-4	9.35e-4
V	2.81e-2	5.49e-1	4.66e-3	2.30e-3	2.75e-2	4.56e-3	1.64e-3	1.49e+0	4.64e+1	2.12e+1	2.59e+0	6.04e-3	9.35e-4
$\tilde{\theta}$	3.52e-4		1.23e+0	9.96e-1	2.74e-2	1.00e+0	6.17e-3	3.31e-3		2.26e-4	2.42e-5	1.57e-1	1.00e+0
E	3.09e-6		1.46e-3	1.82e-3	1.37e-4	1.19e-3	4.11e-6	1.43e-3		1.75e-3	7.48e-6	4.59e-4	3.53e-4
V	8.78e-3		1.19e-3	1.83e-3	4.99e-3	1.19e-3	6.67e-4	4.31e-1		7.75e+0	3.09e-1	2.94e-3	3.53e-4
$\tilde{\theta}$			1.23e+0	9.96e-1	2.73e-2	9.97e-1	6.16e-3	3.27e-3			2.15e-5	1.59e-1	9.96e-1
E			1.41e-3	1.72e-3	1.30e-4	1.11e-3	3.94e-6	1.76e-4			6.92e-6	4.13e-4	3.32e-4
V			1.15e-3	1.73e-3	4.73e-3	1.12e-3	6.39e-4	5.37e-2			3.21e-1	2.60e-3	3.33e-4
$\tilde{\theta}$			1.23e+0		2.73e-2	9.97e-1	6.16e-3				1.85e-5	1.59e-1	9.96e-1
E			1.39e-3		1.13e-4	1.06e-3	1.85e-6				1.23e-6	3.71e-4	1.04e-4
V			1.13e-3		4.14e-3	1.06e-3	3.00e-4				6.64e-2	2.33e-3	1.04e-4
$\tilde{\theta}$					2.68e-2	9.98e-1	6.15e-3				1.98e-05	9.97e-1	9.97e-1
E					1.94e-5	2.28e-5	1.35e-6				1.24e-06	4.57e-5	4.57e-5
V					7.25e-4	2.28e-5	2.20e-4				6.24e-02	4.59e-5	4.59e-5
$\tilde{\theta}$					2.68e-2	9.99e-1	6.15e-3					9.98e-1	9.98e-1
E					1.87e-5	2.27e-5	1.33e-6					4.55e-5	4.55e-5
V					7.01e-4	2.27e-5	2.16e-4					4.57e-5	4.57e-5
$\tilde{\theta}$						9.98e-1	6.16e-3					9.97e-1	9.97e-1
E						2.26e-5	1.33e-6					4.51e-5	4.51e-5
V						2.26e-5	2.15e-4					4.53e-4	4.53e-4

Table 6: Parameter estimates for solving seven inverse problems from a synthetic data generated using the given nominal parameters and variance. For each parameter subset, we display the estimate ($\tilde{\theta}$), the standard error, E and the coefficient of variation, $V = E/\tilde{\theta}$.

θ	California	Florida	Georgia	Maryland	Texas	Washington	Wisconsin
b_1	1.0000e-15	1.0000e-15	4.6495e-02	1.0080e-05	1.4196e-05	2.0116e-02	1.0000e-15
β_A	8.8973e-05	9.8043e-01	1.0939e+00	1.3360e+00	5.6047e-01	9.5295e-01	6.3325e-01
β_S	1.1213e+00	6.9601e-01	5.1042e-01	1.3320e+00	1.1989e-02	1.0000e+00	1.0773e+00
σ	9.9999e-01	1.0000e+00	7.5663e-01	1.0000e+00	1.0000e+00	7.3519e-01	7.1669e-01
γ_1	3.5769e-02	8.3577e-01	9.8459e-01	9.9686e-01	1.2284e-01	8.9911e-01	1.0000e+00
γ_2	9.1747e-01	7.8446e-01	7.6914e-01	9.6675e-01	6.6645e-02	8.9098e-01	1.0000e+00
ρ	1.3366e-07	1.0000e-15	1.0000e-15	4.5126e-05	5.4691e-02	2.9082e-06	1.0325e-03
μ_1	2.7409e-03	6.7600e-09	6.5427e-04	6.6585e-04	1.0000e-15	6.9886e-04	8.7380e-04
μ_2	1.1988e-05	8.1025e-04	3.4154e-04	1.0000e-15	1.2534e-02	3.1211e-06	8.6293e-02
μ_3	6.8398e-05	6.9384e-05	3.2020e-08	1.0000e-15	1.0000e-15	3.6933e-06	6.0737e-04
μ_4	1.0000e-15	1.0000e-15	1.0000e-15	.0000e-15	1.0000e-15	1.2343e-05	1.0000e-15
η	1.1097e-01	9.4378e-01	1.0000e+00	9.9986e-01	3.0315e-01	3.9910e-01	4.6680e-05
α	9.9980e-01	8.7834e-01	9.9967e-01	7.7423e-01	9.8525e-01	1.0000e+00	1.0000e+00
T^*	150	110	110	110	130	150	140

Table 7: Model fit parameters for some selected states in the US, T^* shows the number of days used for each state.